

PL
CR

TECHNICAL NOTE

D-1467

49932

ON SCALING LAWS FOR MATERIAL DAMPING

Stephen H. Crandall

Massachusetts Institute of Technology

DISTRIBUTION STATEMENT A

Approved for Public Release
Distribution Unlimited

PROPERTY OF:
AMPTIAC LIBRARY

2001129079

NATIONAL AERONAUTICS AND SPACE ADMINISTRATION
WASHINGTON

December 1962

Reproduced From
Best Available Copy

ON SCALING LAWS FOR MATERIAL DAMPING

by
Stephen H. Crandall
Massachusetts Institute of Technology

SUMMARY

ES, A
Similarity analyses are made to provide scaling laws which indicate the effects of amplitude, frequency, and material properties on the resonant damping experienced by structural elements when the damping is due to internal material properties. Two nonlinear damping "laws" are considered. The first concerns frequency-independent hysteresis damping in which the material damping coefficient g satisfies a relation of the form

$$g = \left(\frac{S}{S_0}\right)^n , \quad (i)$$

where S is the stress amplitude and S_0 and n are material constants. The second damping law concerns nonlinear damping for which

$$g = \left(\frac{S}{S_0}\right)^n \frac{\omega\tau}{1 + \omega^2\tau^2} , \quad (ii)$$

with the relaxation time τ being an additional material constant. Correlations provided by the scaling laws were performed on data from a large number of tests with steel, brass and aluminum cantilever beams. The steel and brass data were correlated reasonably well on the basis of (i) while the aluminum data were better correlated on the basis of (ii). *end*

CONTENTS

Summary	i
Foreword	vi
INTRODUCTION	1
INTERNAL DAMPING BY LINEAR RELAXATION PROCESSES	2
SIMILARITY ANALYSIS FOR NONLINEAR FREQUENCY- INDEPENDENT HYSTERESIS DAMPING	3
SIMILARITY ANALYSIS FOR A NONLINEAR RELAXATION PROCESS	9
EXPLICIT ANALYSIS FOR A CANTILEVER BEAM	10
CORRELATION OF EXPERIMENTAL DATA	14
CONCLUSIONS	21

FOREWORD

This technical note represents the first of a series that will be published covering work sponsored by the Marshall-Goddard* Vibration Committee. This Committee utilizes results from previous research and extends these findings with the following specific objectives:

1. To advance technical knowledge in such a way that vibration test specifications gradually will improve and will take into account non-linear behavior of the materials generally used in spacecraft construction.
2. To postulate more realistic assumptions regarding the nature of the random and quasi-periodic oscillations usually encountered in spacecraft structures (those which ensue from more complex or random external excitation). Obviously, specifications then may be written with less margin of error between true structural inputs and their laboratory-simulated counterparts.

With regard to the results published herein, formulas evolved from the theory have not, as yet, been verified through carefully planned new experimentation. However such experimentation now is being prepared at Goddard Space Flight Center. The results from this experimental study would be expected to define certain limitations within which the Author's findings may be employed.

*Marshall Space Flight Center, Huntsville, Alabama; and Goddard Space Flight Center, Greenbelt, Maryland.

ON SCALING LAWS FOR MATERIAL DAMPING*

by

Stephen H. Crandall

Massachusetts Institute of Technology

INTRODUCTION

Possibly the most vexing problem in mechanical vibrations is that of damping. Generally speaking, it is only in lightly damped systems that vibration becomes a critical factor. There are, however, a multitude of mechanisms which produce small amounts of damping and our knowledge about many of them is far from adequate. The present investigation is limited to vibrations of single continuous metal elements such as beams. When such an element vibrates, damping may arise externally owing to windage or to acoustical transmission of energy because the vibration takes place in air; and it may arise as a result of slippage at, or of energy transmission across, an interface where the element is connected to the exciter or to a foundation. In addition, damping will arise within the element itself because of the fluctuating stress-strain history. The relative importance of internal vs. external damping varies widely with the application. We shall be concerned here with the case where the internal damping is overriding. This will be the case if, for example, the vibration takes place in a vacuum and the connections of the element are such as to minimize the possibility of slip damping and energy loss across the interface.

This investigation was undertaken to rationalize certain anomalous results obtained by Granick¹ from tests on clamped cantilever reeds. A similarity analysis of nonlinear hysteresis damping (see Section 2) was made which appeared to show promise as a means of correlating the results. At this time a more extensive set of similar test results was made available by Vet². The proposed correlation appeared to be satisfactory for steel and brass but quite unsatisfactory for aluminum (see Section 5). As a result, a further similarity analysis was made of a nonlinear relaxation process (see Section 3) which led to a reasonably good correlation for the aluminum data.

*Manuscript submitted December 1961

¹Granick, N., "Choosing a Suitable Sweep Rate for Sinusoidal Vibration Testing," NASA Technical Note D-709, October 1961

²Vet, M., Collins Radio Company, Cedar Rapids, Iowa (private communication). See also "Study Program to Modify the Vibration Requirements of MIL-T-5422E and MIL-E-5272C (Dwell-Sweep Correlation Study)", Collins Engineering Report 1582, May, 1962.

INTERNAL DAMPING BY LINEAR RELAXATION PROCESSES

Linear relaxation processes in metals have been surveyed by Zener³, who described a number of different mechanisms. Of those which have received quantitative attention the only one which is significant at room temperature, in the frequency range of importance in mechanical vibration (1 to 10,000 cps), is the mechanism of relaxation by transverse thermal currents. The amount of damping provided is, however, somewhat smaller than is generally found in vibrations involving engineering stress levels. It is nevertheless of interest to review the theory of this mechanism.

Let us consider a metal reed vibrating transversely. When the fibers at one side are stretched, they tend to cool; and the fibers at the other side, which are compressed, tend to heat. The difference in temperature causes a thermal current to flow across the beam, which involves some irrecoverable loss in energy. The amount of the loss depends critically on the time factors involved. If the beam vibrates at a very high frequency, the alternate heating and cooling of the fibers is so rapid that it is essentially adiabatic and very little heat flows transversely. On the other hand, if the frequency is low enough the change in temperature of the fibers is so slight that again there is very little transverse heat transfer. Between these extremes there is a condition of maximum loss and maximum damping. It is of interest to examine the precise nature of the dependence of the damping on the frequency in this process.

It is shown by Zener³ that for simple harmonic motion at frequency ω the dynamic tension modulus in a bending beam may be taken in the complex form $E(1 + ig)$ with the damping coefficient g given by

$$g = \frac{\alpha^2 ET}{c} \frac{\omega\tau}{1 + \omega^2\tau^2} \quad (1)$$

where

- α = linear expansion coefficient,
- E = tension modulus,
- T = absolute temperature,
- c = specific heat per unit volume,

and τ is the relaxation time for the equalization of temperature in the beam by transverse heat flow. The evaluation of τ for any specific shape of beam cross-section requires the solution of a difficult heat transfer problem. For a flat reed of uniform thickness, Zener³ gives the following result:

$$\tau = \frac{h^2 c}{\pi^2 k} \quad (2)$$

³Zener, C. M., "Elasticity and Anelasticity of Metals," Chicago: University of Chicago Press, 1948

where h is the thickness of the reed, k is the thermal conductivity, and k/c is known as the thermal diffusion coefficient. The frequency dependence in Equation 1 should be noted: the damping coefficient is maximum at the frequency $\omega = 1/\tau$ and falls off gradually to zero for both very high and very low frequencies. The result given by Equation 1 is due to a single relaxation mechanism. Actually there are a number of such mechanisms, each with its own relaxation time τ . Because of the linearity they can simply be superposed to provide the total damping coefficient. If the relaxation times for the different mechanisms are separated by orders of magnitude (as is usually the case), then it is possible to consider each mechanism separately in the frequency range (about two decades) in which it peaks.

In Figure 1 curves of damping coefficient vs. frequency according to Equation 1 have been plotted for 1/16-inch-thick reeds of steel (0.2% C, cold rolled); brass (1/2 hard, yellow); and aluminum (2024-T4); all at room temperature. To obtain these results the values given in Table 1 were employed.

It should be noted that for frequencies considerably higher than the frequency $\omega = 1/\tau$ where the peak occurs, the variation of the damping coefficient is very nearly inversely proportional to ω according to Equation 1. It should also be emphasized that the theory involved is *linear*, i.e., according to this model the damping coefficient should be independent of the amplitude of vibration.

SIMILARITY ANALYSIS FOR NONLINEAR FREQUENCY- INDEPENDENT HYSTERESIS DAMPING

A striking property of internal damping of vibration in metals at engineering stress levels is its nonlinearity with respect to amplitude⁴; and in some cases there is little, if any, frequency dependence throughout the range of engineering importance. It is commonly assumed that the damping coefficient g varies as a power of the stress amplitude S ; i.e., that

$$g = \left(\frac{S}{S_0}\right)^n , \quad (3)$$

where S_0 and n are material constants. Data for many metals⁵ appear to fit this relation, with n falling between zero and unity when the stress level is below a certain critical stress that is quite close to the fatigue strength of the material. Above this limit the damping

⁴See, for example, Pian, T. H. H., "Structural Damping," in: *Random Vibration*, ed. by S. H. Crandall, Cambridge: Technology Press of the Massachusetts Institute of Technology, 1958, Chapter 5

⁵Lazan, B. J., and Goodman, L. E., "Material and Interface Damping," in: *Shock and Vibration Handbook*, ed. by C. M. Harris and C. E. Crede, New York: McGraw-Hill, 1961, Vol. 2, Chapter 36.

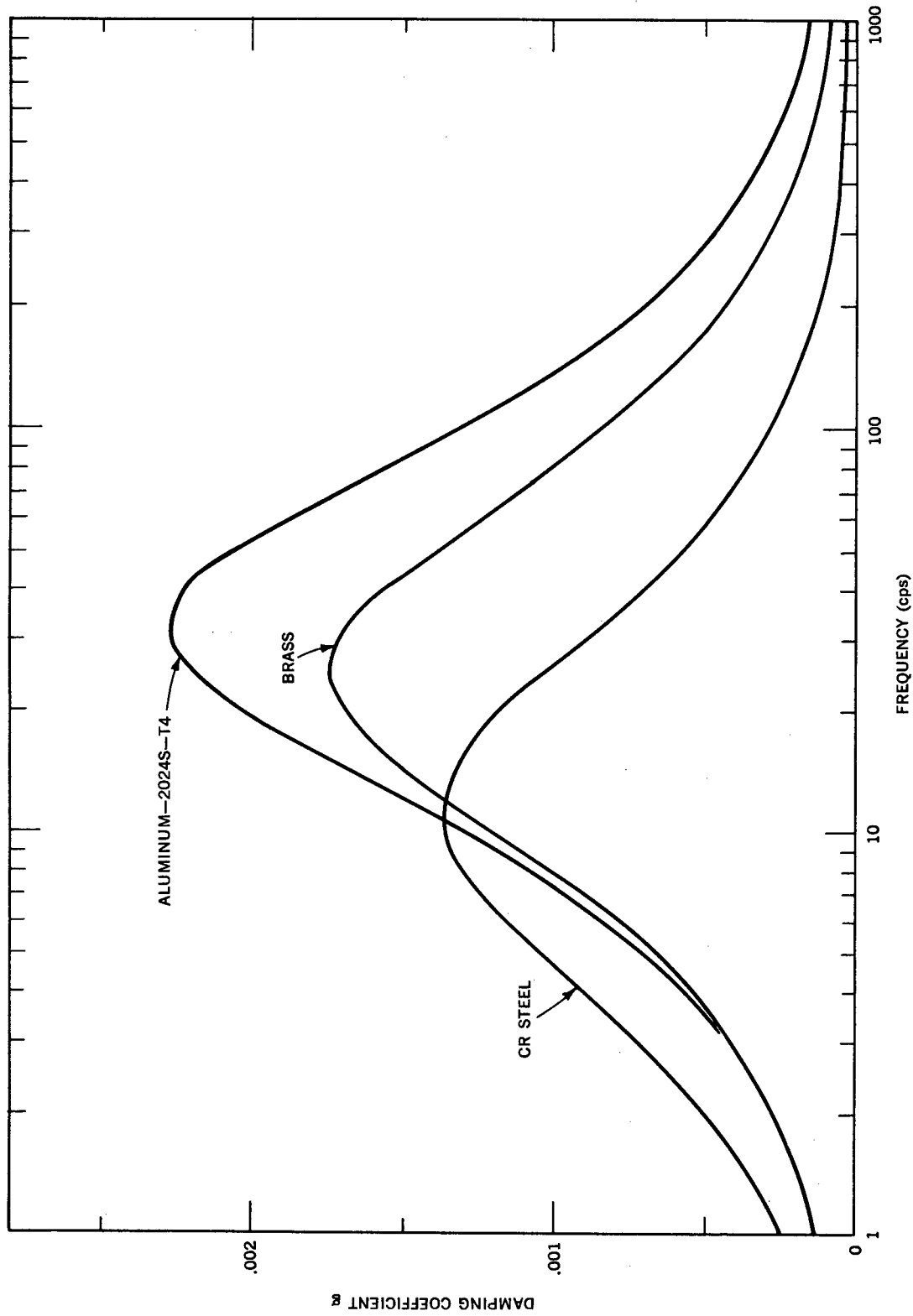


Figure 1—Damping due to transverse thermal currents as a function of vibration frequency (at room temperature)

Table 1
Values Used in Equation 1 to Obtain the Curves Shown in
Figure 1; All Data Taken at Room Temperature

Reed Material	α (strain) $(^{\circ}\text{F})$	E (psi)	c (psi) $(^{\circ}\text{F})$	k (lb sec $(^{\circ}\text{F})$)	k/c (in ²) sec
Steel	6.7×10^{-6}	30×10^{-6}	245	6.5	0.027
Brass	10.5×10^{-6}	15×10^{-6}	230	14.9	0.063
Aluminum	12.9×10^{-6}	10.6×10^{-6}	197	15.8	0.080

becomes dependent on the stress history, and values of $n = 20$ or more are possible. It is commonly assumed that the physical mechanism behind Equation 3 is plastic action as slip-planes and dislocations migrate back and forth; but a quantitative theory appears to be lacking.

We shall now make a similarity analysis of such damping when a metal body is vibrated at a natural frequency by a simple harmonic driver. We consider a family of geometrically similar bodies with a characteristic length dimension L . The elastic constants E and ν are assumed to remain constant independently of the vibration amplitude; i.e., the vibratory system is considered to be *linear* in all respects except for the damping coefficient, Equation 3, which is assumed to be small. Furthermore, although the continuous body has infinitely many degrees of freedom, we can limit our analysis to a *single degree of freedom* by restricting our consideration to a single mode of vibration (e.g., the fundamental). When the body is excited at the corresponding natural frequency, the response consists overwhelmingly of this mode alone; and the lighter the damping the more true this becomes.

The first step is to note how the natural frequency varies with changes in the characteristic length L . Let

$$\begin{aligned}\omega_n &= \text{natural frequency,} \\ E &= \text{modulus of elasticity,} \\ \nu &= \text{Poisson's ratio,} \\ \rho &= \text{mass density.}\end{aligned}$$

Then by dimensional analysis or by observing the known formulas for simple bodies (beams, etc.) we have

$$\omega_n = \frac{1}{L} \sqrt{\frac{E}{\rho}} f(\nu, \text{shape}) \quad (4)$$

By restricting ourselves to geometrically similar bodies we need not take the shape factor into account for purposes of scaling. However, Poisson's ratio ν is more troublesome.

In order to proceed in a simple manner we will make the further assumption that either all materials to be considered have the same value of Poisson's ratio or that the mode of vibration is such (e.g., in a slender member) that Poisson's ratio does not appear in Equation 4. In either case Equation 4 simplifies to

$$\omega_n \sim \frac{1}{L} \sqrt{\frac{E}{\rho}} . \quad (5)$$

If the mode is such that twisting or shearing clearly predominates we will use the shear modulus G , in place of E in Equation 5.

The assumption has been made that the damping is sufficiently small to have no effect on the natural frequency. We also assume that the mode *shape* is unaffected by the damping. The damping does, however play a crucial role in fixing the *amplitude* of the mode when the body is excited at resonance. Let δ be a characteristic deflection of the mode. Then the amplification factor at resonance is given by

$$Q = \frac{\delta_{res}}{\delta_0} , \quad (6)$$

where the deflections are due to distributed exciting forces proportional to the inertia forces of the mode in question. In one case this distribution of forces is applied statically to give δ_0 and in the other case the same pattern of force amplitudes occurs in simple harmonic motion at the natural frequency. A necessary preliminary in reducing this to a single degree of freedom is to decompose the actual excitation pattern into natural mode components and to disregard all contributions except that of the mode in question. In any particular case in which a quantitative comparison between theory and experiment is required (an example of this is shown in Section 4), the mode participation factor will have to be calculated. For purposes of scaling, the actual value of the mode participation factor is unnecessary because it remains fixed for geometrically similar cases.

The next step is to relate the deflections to the excitation. A simple way to obtain the form of the results is to consider the single-degree-of-freedom model shown in Figure 2: Let us take the excitation to be a forced motion of the foundation characterized by the amplitude a of the *acceleration*. The static and resonant deflections can be obtained from a dynamical analysis. The mass m represents the effective inertia for the mode in question, and the complex spring constant $k(1 + ig_s)$ represents the effective stiffness for the same mode resulting from the configuration and from the complex modulus $E(1 + ig)$. The relation between the *specimen damping coefficient* g_s and the material damping coefficient g is of the form

$$g_s = g R(n, \text{mode shape}) , \quad (7)$$

where the dimensionless ratio R depends on the configuration of the body, on the particular mode under consideration, and on the exponent n in the damping "law" (Equation 3). General procedures for obtaining R have been outlined by Lazan and Goodman⁵ and an explicit expression for a cantilever beam is derived here in Section 4. For *linear* damping mechanisms in homogeneous bodies, the ratio R is unity and the specimen damping coefficient is identical with the material damping coefficient.

In Figure 2 the amplitude of the foundation acceleration is a and the deflection δ is the relative displacement of the mass with respect to the foundation. When the foundation acceleration is applied statically (i.e., unidirectional steady acceleration of magnitude a) the inertia force on the mass is $-ma$ and the steady state deflection is

$$\delta_0 = \left| \frac{-ma}{k} \right| = \frac{a}{\omega_n^2}, \quad (8a)$$

where $\omega_n = \sqrt{k/m}$ is the natural frequency of the mode in question. When the foundation's motion is at the resonant frequency, the amplitude of the resonant deflection is

$$\delta_{res} = \left| \frac{-ma}{k(1 + ig_s) - m\omega_n^2} \right| = \frac{a}{g_s \omega_n^2}. \quad (8b)$$

Comparison of these results with Equation 6 shows that

$$Q = \frac{1}{g_s}. \quad (9)$$

It remains to relate the specimen damping coefficient to the resonant deflection. According to Equation 3 the damping depends nonlinearly on the stress amplitude. The stress, however, depends linearly on the strain which in turn depends linearly on the deflection. In fact, since strain is change in length (which is proportional to δ) divided by original length (which is proportional to L), we have

$$S \sim E \frac{\delta_{res}}{L} \quad (10)$$

for the resonant stress amplitude. Equations 3, 5, 7, and 10 can now be combined as follows:

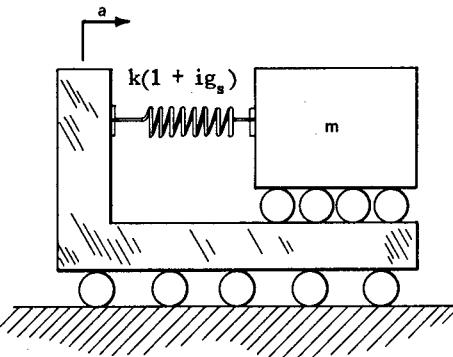


Figure 2—Single-degree-of-freedom model for analyzing the response of a single vibration mode of a continuous member

$$\begin{aligned}
 g_s &= R \left(\frac{S}{S_0} \right)^n \sim R \left(\frac{E}{S_0} \frac{\delta_{res}}{L} \right)^n \\
 &\sim R \left(\frac{E \omega_n \delta_{res}}{S_0 \sqrt{\frac{E}{\rho}}} \right)^n \\
 &\sim R \left(\frac{\sqrt{\rho E}}{S_0} \omega_n \delta_{res} \right)^n . \quad (11)
 \end{aligned}$$

Finally introducing Equation 8b, we have

$$g_s \sim R \left(\frac{\sqrt{\rho E}}{S_0} \frac{a}{\omega_n} \frac{1}{g_s} \right)^n , \quad (12)$$

from which we obtain the scaling law for the damping coefficient g_s :

$$g_s \sim R^{\frac{1}{n+1}} \left(\frac{\sqrt{\rho E}}{S_0} \frac{a}{\omega_n} \right)^{\frac{n}{n+1}} . \quad (13)$$

Note that ρ , E and S_0 are material constants (as is n) while a indicates the level of the excitation; and since we are confined to considering a particular mode of vibration, ω_n is essentially a size parameter whose value characterizes one of a family of geometrically similar bodies. The amplification at resonance, Q , is simply the reciprocal of g_s , so its scaling law is

$$Q = \left(\frac{1}{R} \right)^{\frac{1}{n+1}} \left(\frac{S_0}{\sqrt{\rho E}} \frac{\omega_n}{a} \right)^{\frac{n}{n+1}} . \quad (14)$$

Although these results have been derived for complete geometric similarity they apply to a somewhat wider class of cases. For example they apply to uniform one-dimensional members, such as beams and shafts, where the cross section is fixed and only the longitudinal dimension is altered. In fact, they apply to any family of shapes in which the resonant stress amplitude is related to the resonant velocity amplitude $\omega_n \delta_{res}$ by an expression of the form⁶

$$S \sim \sqrt{E\rho} \omega_n \delta_{res} . \quad (15)$$

If this equation holds, then Equation 13 is valid even when Equations 5 and 10 assume different forms.

⁶For an enumeration of several such cases see Hunt, F. V., "Stress and Strain Limits on the Attainable Velocity in Mechanical Vibration," *J. Acoust. Soc. Amer.* 32(9):1123-1128, September 1960. Apparently the fact that resonant stress is proportional to resonant velocity was first recognized by H. G. Yates in "Vibration Diagnoses in Marine Geared Turbines," *Trans. North East Coast Institution of Engineers and Shipbuilders*, 65, pt. 4:225-261, February 1949, Appendix I.

SIMILARITY ANALYSIS FOR A NONLINEAR RELAXATION PROCESS

In Section 1 the frequency dependence of the damping coefficient for a single linear relaxation phenomenon was seen to be of the form

$$g \sim \frac{\omega\tau}{1 + \omega^2\tau^2}, \quad (16)$$

while in Section 2 the implications of the nonlinear frequency-independent relation

$$g = \left(\frac{S}{S_0}\right)^n \quad (17)$$

were examined. In this section we consider the consequences of a hypothetical mechanism having the frequency dependence of Equation 16 and the amplitude dependence of Equation 17; i.e., we consider a nonlinear-relaxation damping mechanism for which

$$g = \left(\frac{S}{S_0}\right)^n \frac{\omega\tau}{1 + \omega^2\tau^2}, \quad (18)$$

where n , S_0 and τ are material constants. The microscopic mechanism responsible for Equation 18 is not hypothesized at present; it is therefore an *ad hoc* relation. We will see, however, that experimental data for aluminum correlate better with Equation 18 than with 17.

We next make a similarity analysis based on Equation 18 for a family of similarly shaped bodies being driven at resonance in a given mode of vibration. The analysis is almost identical with that in Section 2 except for the replacement of Equation 3 by the new assumption 18. It is only necessary to eliminate S and δ_{res} from Equations 8, 15, and 18 to obtain

$$g_s = \left[R \left(\frac{\sqrt{\rho E}}{S_0} a \right)^n \frac{\omega_n \tau}{\omega_n^n (1 + \omega_n^2 \tau^2)} \right]^{\frac{1}{n+1}} \quad (19)$$

as the scaling law for the specimen damping coefficient g_s . The material constants are ρ , E , S_0 , τ and n , while a is a measure of the amplitude of the input acceleration and ω_n is the natural frequency of the mode in question.

If the relaxation phenomenon Equation 18 peaks at a frequency $1/\tau$ which is low compared to any of the resonant frequencies ω_n to be considered, then $\omega_n \tau$ would always be large compared to unity and Equation 18 could be simplified by omitting the 1 in the denominator. In that case Equation 19 takes the simplified form

$$g_s \approx \left[R \left(\frac{\sqrt{\rho E}}{S_0} a \right)^n \frac{1}{\tau \omega_n^{n+1}} \right]^{\frac{1}{n+1}}. \quad (20)$$

Finally, if in addition we concentrate on a fixed material and consider only changes in size and in excitation level, the scaling law (Equation 20) reduces to the relation

$$g_s \omega_n \sim a^{\frac{n}{n+1}}. \quad (21)$$

EXPLICIT ANALYSIS FOR A CANTILEVER BEAM

Similarity analyses were used to obtain the scaling laws (Equations 13 and 19) for nonlinear frequency-independent damping and for damping due to a nonlinear relaxation process. In this section we verify these general results for a particular case in which exact analysis is possible.

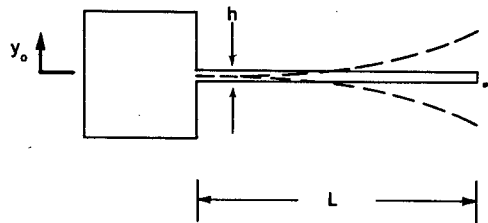
We consider the cantilever beam or reed shown in Figure 3 when the base is driven sinusoidally with acceleration amplitude a at the fundamental resonant frequency of the beam.

We will derive explicit relations for the specimen damping coefficient g_s in terms of the two hypothetical nonlinear damping "laws" already used⁷.

Let $v(x, t)$ be the relative transverse deflection of the beam and consider first the free undamped motion. The differential equation is

$$EI \frac{\partial^4 v}{\partial x^4} + \rho b h \frac{\partial^2 v}{\partial t^2} = 0, \quad (22)$$

Figure 3—Cantilever beam of length L and depth h excited by motion $y(t)$ of the base



where EI is the flexural modulus, ρ the mass density, b the width, and h the depth of the beam. This equation, together with the boundary conditions for a cantilever, fixes the natural modes $\phi_m(x)$ and the natural frequencies ω_m . These have been tabulated⁸. The first mode of the cantilever is

$$\phi_1(x) = \cosh \lambda_1 x - \cos \lambda_1 x - \sigma_1 (\sinh \lambda_1 x - \sin \lambda_1 x), \quad (23)$$

⁷A similar result for the damping law of Equation 3 has been obtained by J. Wilkening of the Brown Engineering Company, Huntsville, Alabama (private communication).

⁸Young, D., and Felgar, P. R., Jr., "Tables of Characteristic Functions Representing Normal Modes of Vibration of a Beam," Austin: University of Texas, 1949 (Univ. Texas Publ. No. 4913; Eng. Res. Ser. No. 44); See also Bishop, R. E. D., and Johnson, D. C., "The Mechanics of Vibration," Cambridge: The University Press, 1960, p. 382.

where

$$\begin{aligned}\lambda_1 L &= 1.8751, \\ \sigma_1 &= 0.7341;\end{aligned}\quad (24)$$

and the corresponding natural frequency ω_1 is given by

$$\omega_1^2 = \frac{EI \lambda_1^4}{\rho bh} = 12.36 \frac{EI}{\rho bh L^4}. \quad (25)$$

We next consider the steady deflection of the beam when the base is steadily accelerated with the constant acceleration a . The loading is the inertia force ρbha per unit length, and the governing equation for the deflection $v(x)$ is

$$EI \frac{d^4 v}{dx^4} = \rho bha. \quad (26)$$

This deflection may be considered as a superposition of all the natural modes

$$v(x) = \sum C_m \phi_m(x). \quad (27)$$

In order to measure the amplification factor at the resonance of mode ϕ_1 we need to know the magnitude of C_1 in Equation 27. This is found by inserting 27 into 26, multiplying both sides by $\phi_1(x)$, and integrating over the length of the beam. Using the orthogonality of the modes, together with the fact that the natural modes satisfy

$$EI \frac{d^4 \phi_m}{dx^4} = \rho bh \omega_m^2 \phi_m, \quad (28)$$

yields

$$\begin{aligned}C_1 &= \frac{a}{\omega_1^2} \frac{1}{L} \int_0^L \phi_1(x) dx \\ &= 0.783 \frac{a}{\omega_1^2}.\end{aligned}\quad (29)$$

The first-mode tip deflection δ_0 under this steady state loading is

$$\begin{aligned}\delta_0 &= C_1 \phi(L) \\ &= 1.566 \frac{a}{\omega_1^2}.\end{aligned}\quad (30)$$

As a matter of interest the first-mode component in Equation 27 is by far the major contribution. The total contribution from all other modes amounts to between 1 and 2 percent of the first-mode deflection.

Finally, the excitation is taken as simple harmonic motion of the base at the resonant frequency ω_1 . The acceleration of the base still has the amplitude a . We assume that the damping is sufficiently small that the response of all other modes is negligible, i.e., the response mode shape is simply $C_{res} \phi_1(x)$. The resonant amplitude of this mode is limited only by the damping.

A convenient procedure for evaluating the effective specimen damping coefficient g_s is based on the relation

$$g_s = \frac{\Delta W}{2\pi W} , \quad (31)$$

where W is the peak potential energy in the oscillation and ΔW is the energy loss per cycle. The calculation for W is independent of the damping mechanism. It consists in integrating the *strain energy per unit volume* $S^2/2E$ throughout the volume of the beam, using the bending stress distribution

$$S = \frac{My}{I} \quad (32)$$

in each cross section with the longitudinal distribution

$$M = EI C_{res} \frac{d^2\phi_1(x)}{dx^2} \quad (33)$$

obtained from the first mode shape. Thus

$$W = \frac{E C_{res}^2}{2} \int_{-\frac{h}{2}}^{\frac{h}{2}} by^2 dy \int_0^L \left(\frac{d^2\phi_1}{dx^2} \right)^2 dx . \quad (34)$$

The integrals in Equation 34 may be made dimensionless by introducing the variables

$$\xi = \frac{x}{L} , \quad \eta = \frac{y}{h} \quad (35)$$

and the notation of Young and Felgar⁸ in which

$$\frac{d^2\phi_1(x)}{dx^2} = \lambda_1^2 \phi_1''(\xi) , \quad (36)$$

where ϕ_1'' is a dimensionless function of the nondimensional variable ξ , and the constant λ_1 is given by Equation 24. In terms of these the peak potential energy is

$$W = \frac{EC_{res}^2}{2} Lbh(h\lambda_1)^2 \int_{-\frac{1}{2}}^{\frac{1}{2}} \eta^2 d\eta \int_0^1 [\phi_1''(\xi)]^2 d\xi. \quad (37)$$

The energy loss per cycle can be obtained from a similar integration in which the *cyclical loss per unit volume* is $2\pi g S^2/2E$ where g is the material damping coefficient. We shall obtain two results from the two hypotheses (Equations 3 and 18) regarding the behavior of g . Using Equation 3 we have

$$\frac{\Delta W}{\text{unit volume}} = 2\pi \left(\frac{S}{S_0}\right)^n \frac{S^2}{2E} \quad (38)$$

which, when integrated throughout the volume, yields

$$\Delta W = 2\pi \frac{EC_{res}^2}{2} \left(\frac{E}{S_0}\right)^n \int_{-\frac{h}{2}}^{\frac{h}{2}} by^{n+2} dy \int_0^L \left(\frac{d^2\phi_1}{dx^2}\right)^{n+2} dx. \quad (39)$$

The integrals in Equation 39 may be cast into dimensionless form by again introducing Equations 35 and 36:

$$\Delta W = 2\pi \frac{EC_{res}^2}{2} \left(\frac{EC_{res}}{S_0}\right)^n Lbh(h\lambda_1^2)^{n+2} \int_{-\frac{1}{2}}^{\frac{1}{2}} \eta^{n+2} d\eta \int_0^1 [\phi_1''(\xi)]^{n+2} d\xi. \quad (40)$$

Finally the specimen damping coefficient g_s is obtained by inserting Equations 37 and 40 into 31. To simplify the result we introduce the symbol R for the following ratio of dimensionless integrals:

$$R = \frac{\int_{-\frac{1}{2}}^{\frac{1}{2}} \eta^{n+2} d\eta \int_0^1 [\phi_1''(\xi)]^{n+2} d\xi}{\int_{-\frac{1}{2}}^{\frac{1}{2}} \eta^2 d\eta \int_0^1 [\phi_1''(\xi)]^2 d\xi}. \quad (41)$$

This ratio depends on the damping "law" exponent n and on the mode shape involved; it can be explicitly evaluated by using the tables of Young and Felgar⁸, but we will not do so here. With this notation the specimen damping coefficient is

$$g_s = R \left(\frac{Eh\lambda_1^2 C_{res}}{S_0}\right)^n. \quad (42)$$

The numerator of the fraction may be recognized as the bending stress amplitude in the extreme fibers at the root of the cantilever during resonance [since $\phi''(0) = 2$]. This permits the further interpretation that R is the ratio of the specimen damping coefficient to the material damping coefficient in the most highly stressed portion of the material. This represents a particular example of the general relation of Equation 7.

The specimen damping coefficient is also related to the amplification at resonance; i.e.,

$$g_s = \frac{C_1}{C_{res}} \quad (43)$$

where C_1 is the amplitude (Equation 29) of the first mode shape under static loading and C_{res} is the amplitude (Equation 42) under resonant loading of the same load amplitude.

Eliminating C_1 and C_{res} among Equations 29, 42, and 43 leads to

$$g_s = R \left(\frac{0.783 a E h \lambda_1^2}{S_0 \omega_1^2 g_s} \right)^n, \quad (44)$$

from which λ_1 can be eliminated by using Equation 25 together with $I = bh^3/12$. This yields

$$g_s = R^{\frac{1}{n+1}} \left(\frac{2.71 \sqrt{\rho E}}{S_0} \frac{a}{\omega_1} \right)^{\frac{n}{n+1}}, \quad (45)$$

which represents an explicit relation for a cantilever beam having the form of the general scaling law of Equation 13.

The analysis based on the nonlinear relaxation "law" (Equation 18) is completely parallel. In place of Equation 45 we find

$$g_s = \left[R \left(\frac{2.71 \sqrt{\rho E}}{S_0} a \right)^n \frac{\omega_1 \tau}{\omega_1^n (1 + \omega_1^2 \tau^2)} \right]^{\frac{1}{n+1}} \quad (46)$$

which is a particular case of the general scaling law of Equation 19.

CORRELATION OF EXPERIMENTAL DATA

The author is grateful to Mr. Maarten Vet of Collins Radio Company for making available a considerable amount of data obtained by vibrating cantilever reeds of steel, brass

and aluminum at room temperature on an electromagnetic shaker². The reeds were 1/16 inch thick and varied from 6-1/2 to 2 inches in length. Care was exercised to minimize losses at the root. The reeds were vibrated in air, however, and the stress levels involved were high. The peak stress at the root was taken well over the fatigue limit in many cases.

The reeds were shaken at their fundamental resonant frequency and the resonant tip amplitude was measured with a microscope as the base acceleration amplitude was varied over a considerable range. The static tip amplitude for the same acceleration was computed from Equation 30 and, when divided by the measured tip amplitude, gave the experimental g_s for the particular material, excitation acceleration amplitude a , and frequency ω_1 .

A preliminary display of the data is shown in Figures 4, 5 and 6 in an effort to separate the stress amplitude and frequency effects. The stress levels indicated are the peak stresses in the reed which occur in the extreme fibers at the root of the cantilever. The data shown in Figures 4, 5 and 6 have been interpolated from Vet's results². Note that for all three materials there appear to be both frequency and amplitude effects, but for steel and brass the amplitude effect is more pronounced than the frequency effect whereas the situation is reversed for aluminum. For comparison, the damping contribution due to relaxation by transverse thermal currents (taken from Figure 1) is also shown in these figures; the smallness of this contribution at engineering stress levels is clearly evident. The frequency range of the data (50 - 500 cps) is insufficient to indicate whether a relaxation phenomenon is responsible for the frequency variations obtained. The data would not be inconsistent with a nonlinear relaxation phenomenon having a peak well below 50 cps.

An attempt to correlate the data by using the scaling law of Equation 13 is shown in Figures 7, 8 and 9. For a given material, this equation yields

$$g_s \sim \left(\frac{a}{\omega_1} \right)^{\frac{n}{n+1}}, \quad (47)$$

so that a log-log plot of g_s vs. a/ω_1 would yield a straight line of slope $n/(n + 1)$. Since the units here are not important, we have simply used gravities (g 's) for the acceleration amplitudes a , and radians/second for the resonant frequencies ω_1 . Note that the correlation is reasonably successful for steel and brass but fails completely for aluminum. For steel the exponent n corresponding to the straight line shown in Figure 7 is 1.26, while for brass the straight line in Figure 8 yields $n = 1.69$. These values might be expected to lie between 0 and 1 if the stress had remained below the cyclic stress sensitivity limit⁵. Actually the stress levels at the root in every specimen went well above this limit.

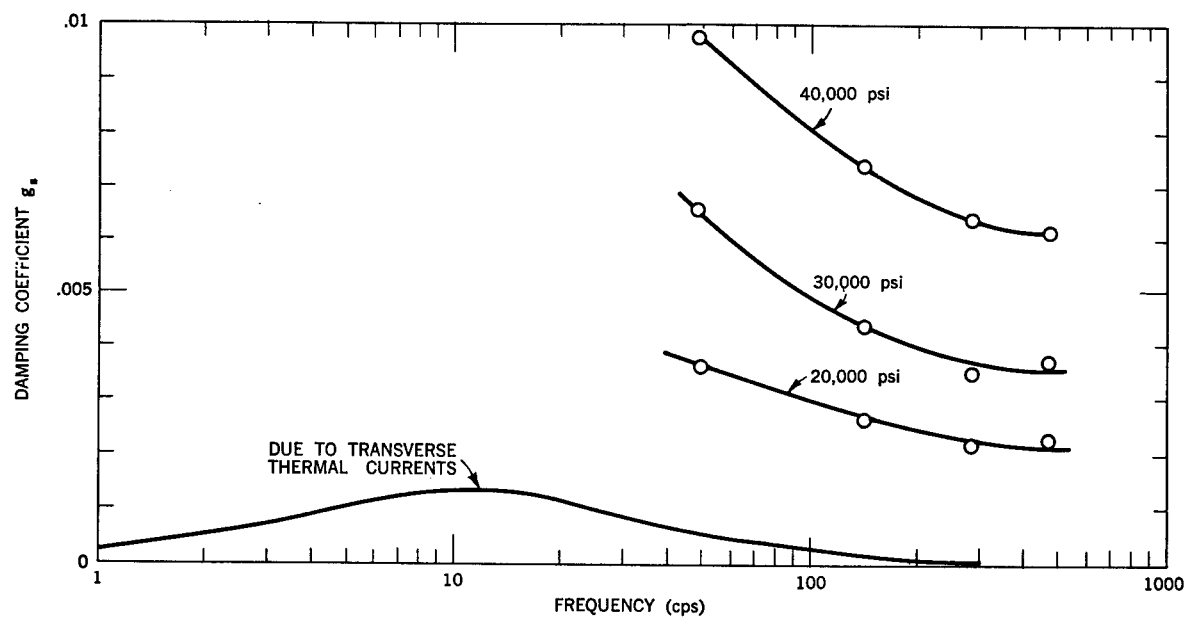


Figure 4—Specimen damping coefficients for cold rolled C1018 steel reeds at constant stress amplitudes

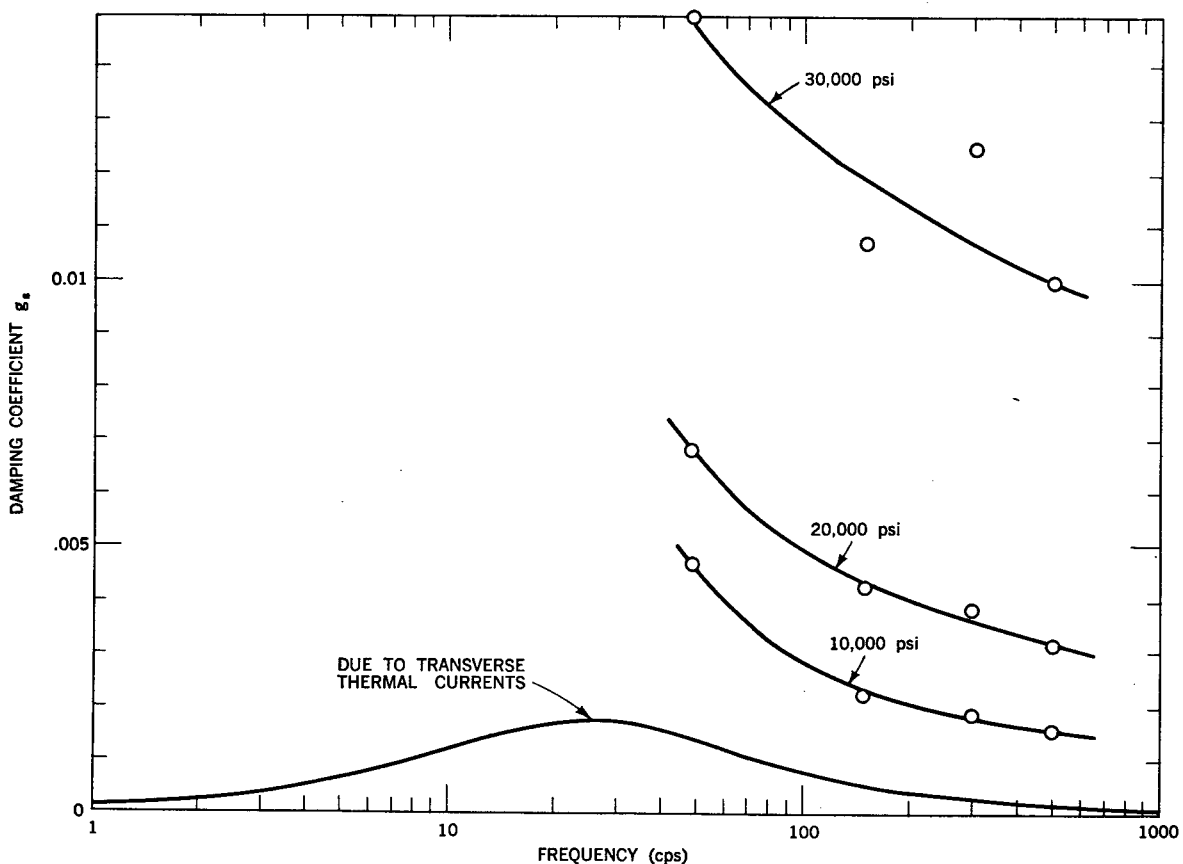


Figure 5—Specimen damping coefficients for free-cutting 1/2-hard brass, at constant stress amplitudes

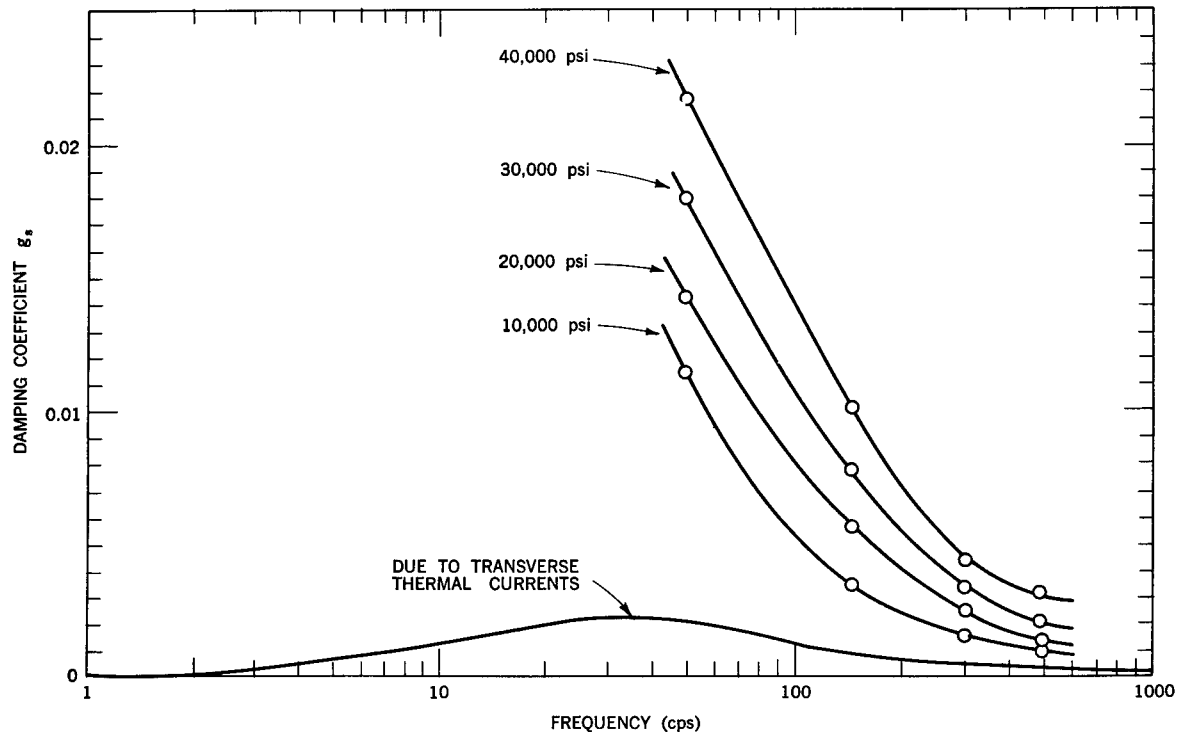


Figure 6—Specimen damping coefficients for 2024-T4 aluminum alloy at constant stress amplitudes

In an attempt to find an improved correlation for the aluminum, a nonlinear relaxation mechanism was postulated in Section 3. This led to the general scaling law of Equation 19. Correlation with this is difficult because of the unknown relaxation time τ . However, the shape of the curves in Figures 4, 5 and 6 suggested that it would be adequate to assume τ large enough so that the approximation of Equation 20 could be used. For a single material this reduces to

$$g_s \omega_1 \sim a^{\frac{n}{n+1}} \quad (48)$$

according to Equation 21. The results of replotted the data on log-log paper with $g_s \omega_1$ as ordinate and a as abscissa are shown in Figures 10, 11, and 12. It is clear from Figures 10 and 11 that the data for steel and brass are *not* satisfactorily correlated by Equation 48. For aluminum, however, the correlation shown in Figure 12 is reasonably satisfactory. From the slope of the straight line shown in Figure 12 we find $n = 0.77$.

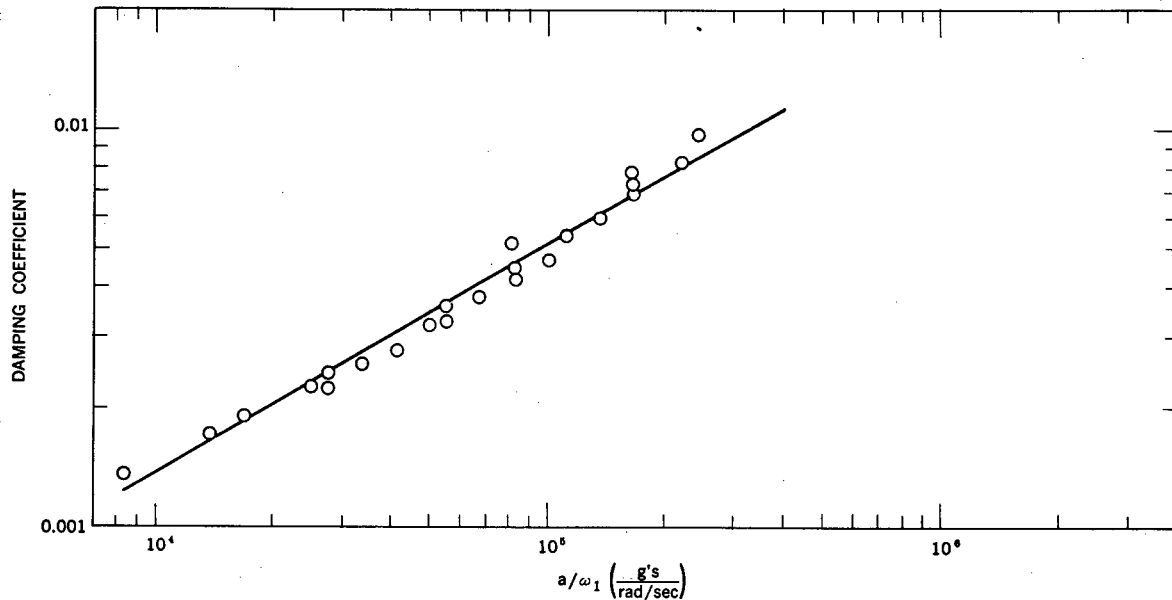


Figure 7—Attempt to correlate damping data for cold-rolled C1018 steel according to Equation 47

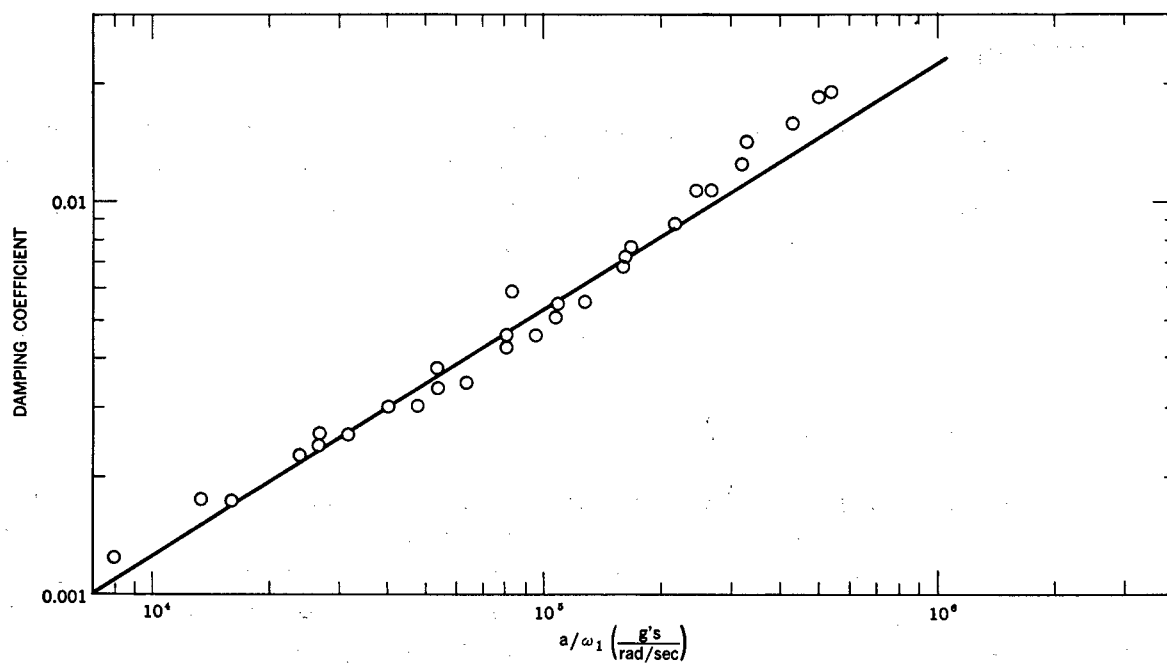


Figure 8—Attempt to correlate damping data for free-cutting 1/2-hard brass according to Equation 47

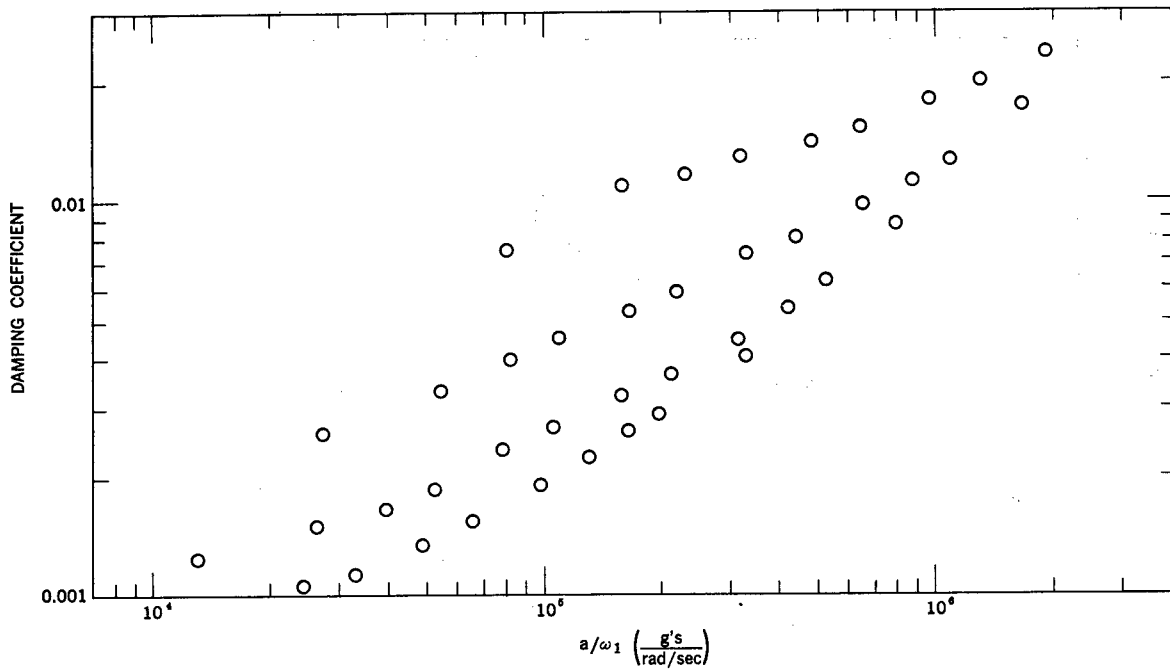


Figure 9—Attempt to correlate damping data for 2024-T4 aluminum alloy according to Equation 47

CONCLUSION

Two nonlinear damping "laws" have been studied and the data from a large number of tests compared with scaling laws derived from these "laws." The assumption of frequency-independent nonlinear damping (Equation 3) gave fair correlation for steel and brass, and the assumption that the damping coefficient satisfies

$$g = \left(\frac{S}{S_0}\right)^n \frac{1}{\omega\tau} \quad (49)$$

gave fair correlation for aluminum.

Actually none of the correlations are perfect. Systematic deviations were noted in every case, and much more work is needed before a clear picture will emerge. The tests should be repeated *in vacuo* to ascertain whether in fact the damping measured was principally due to material damping. Stress levels should be monitored to ascertain whether a simpler pattern exists if the stress levels remain below the cyclic stress sensitivity limit. A wider frequency range would be desirable, perhaps augmented by variation of the temperature.

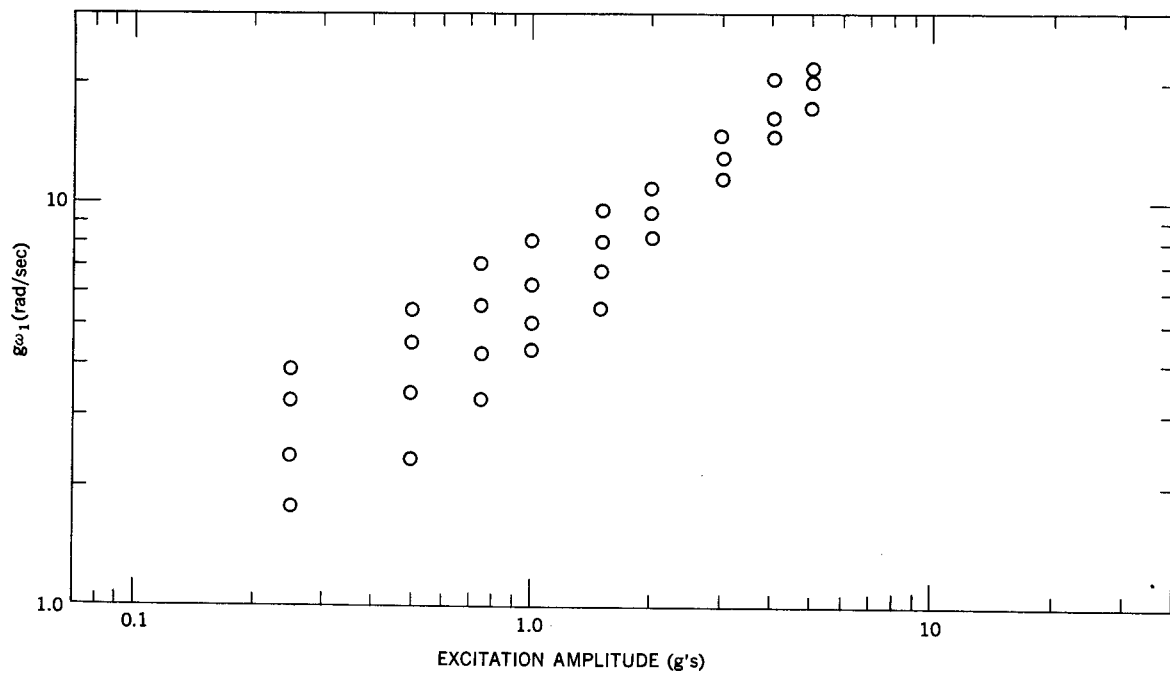


Figure 10—Attempt to correlate damping data for cold-rolled C1018 steel according to Equation 48

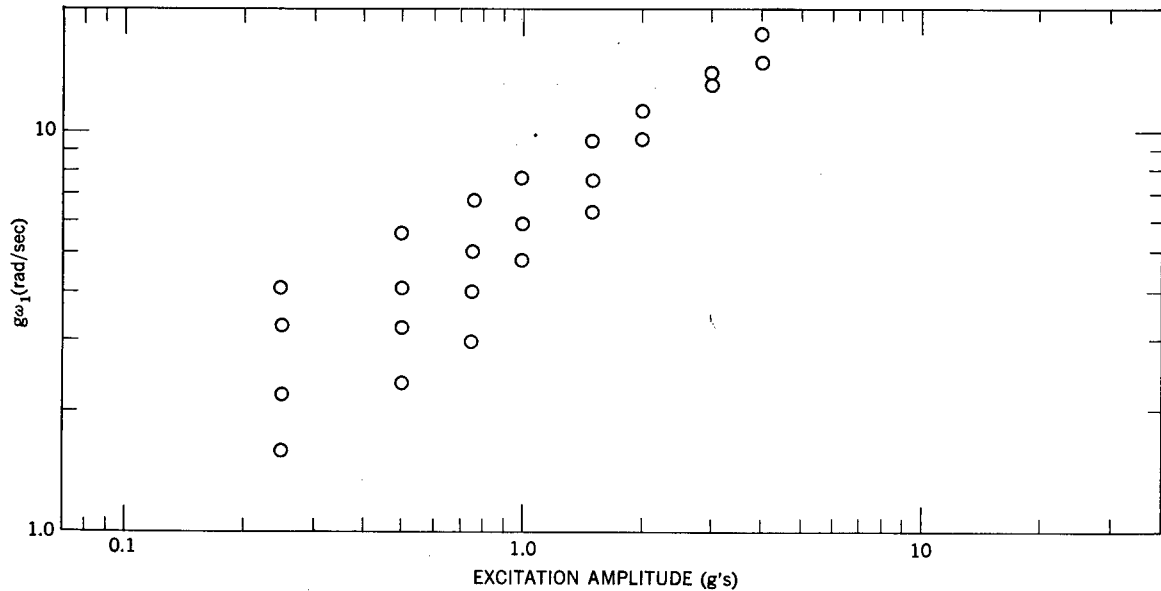


Figure 11—Attempt to correlate damping data for free-cutting 1/2-hard brass according to Equation 48

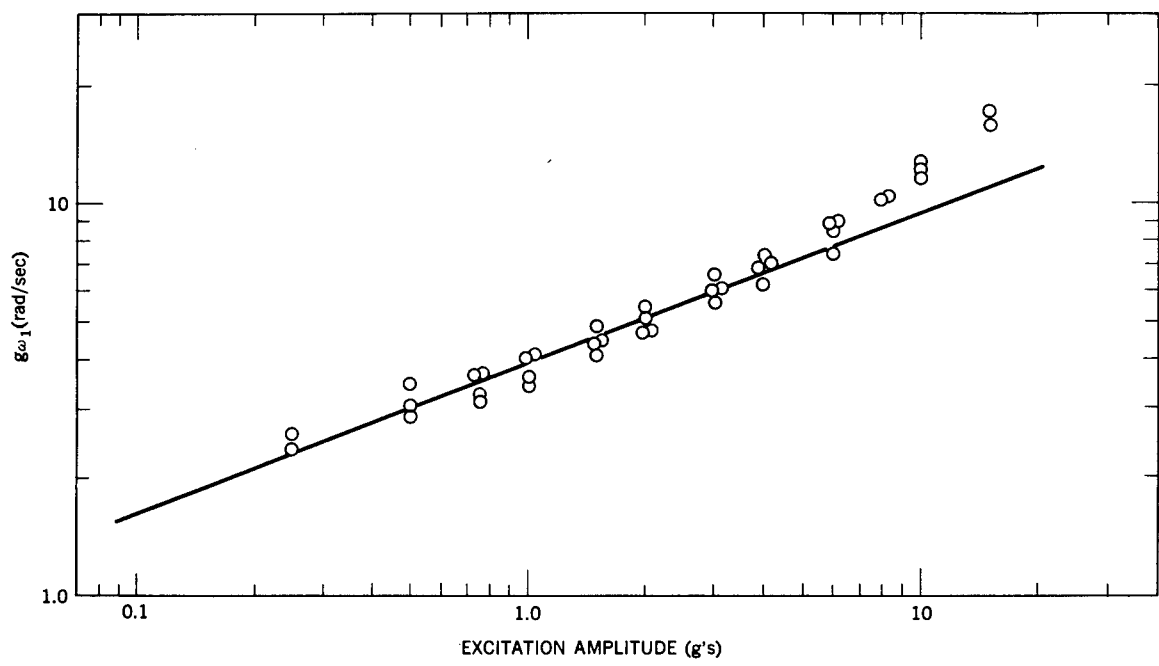


Figure 12—Attempt to correlate damping data for 2024-T4 aluminum alloy according to Equation 48

NASA TN D-1467
National Aeronautics and Space Administration.
ON SCALING LAWS FOR MATERIAL DAMPING.
Stephen H. Crandall, MIT. December 1962. iii, 21p.
OTS price, \$0.75.

(NASA TECHNICAL NOTE D-1467)

Similarity analyses are made to provide scaling laws which indicate the effects of amplitude, frequency, and material properties on the resonant damping experienced by structural elements when the damping is due to internal material properties. Two nonlinear damping "laws" are considered. The first concerns frequency-independent hysteresis damping in which the material damping coefficient g satisfies a relation of the form

$$g = \left(\frac{S}{S_0} \right)^n \quad (1)$$

(over)

NASA

I. Crandall, Stephen H.
II. NASA TN D-1467
III. Mass. Inst. of Tech.
NASA TN D-1467
National Aeronautics and Space Administration.
ON SCALING LAWS FOR MATERIAL DAMPING.
Stephen H. Crandall, MIT. December 1962. iii, 21p.
OTS price, \$0.75.
(NASA TECHNICAL NOTE D-1467)

Similarity analyses are made to provide scaling laws which indicate the effects of amplitude, frequency, and material properties on the resonant damping experienced by structural elements when the damping is due to internal material properties. Two nonlinear damping "laws" are considered. The first concerns frequency-independent hysteresis damping in which the material damping coefficient g satisfies a relation of the form

$$g = \left(\frac{S}{S_0} \right)^n \quad (1)$$

(over)

NASA

I. Crandall, Stephen H.
II. NASA TN D-1467
III. Mass. Inst. of Tech.
NASA TN D-1467
National Aeronautics and Space Administration.
ON SCALING LAWS FOR MATERIAL DAMPING.
Stephen H. Crandall, MIT. December 1962. iii, 21p.
OTS price, \$0.75.
(NASA TECHNICAL NOTE D-1467)

Similarity analyses are made to provide scaling laws which indicate the effects of amplitude, frequency, and material properties on the resonant damping experienced by structural elements when the damping is due to internal material properties. Two nonlinear damping "laws" are considered. The first concerns frequency-independent hysteresis damping in which the material damping coefficient g satisfies a relation of the form

$$g = \left(\frac{S}{S_0} \right)^n \quad (1)$$

(over)

NASA

I. Crandall, Stephen H.
II. NASA TN D-1467
III. Mass. Inst. of Tech.
NASA TN D-1467
National Aeronautics and Space Administration.
ON SCALING LAWS FOR MATERIAL DAMPING.
Stephen H. Crandall, MIT. December 1962. iii, 21p.
OTS price, \$0.75.
(NASA TECHNICAL NOTE D-1467)

Similarity analyses are made to provide scaling laws which indicate the effects of amplitude, frequency, and material properties on the resonant damping experienced by structural elements when the damping is due to internal material properties. Two nonlinear damping "laws" are considered. The first concerns frequency-independent hysteresis damping in which the material damping coefficient g satisfies a relation of the form

$$g = \left(\frac{S}{S_0} \right)^n \quad (1)$$

(over)

NASA

where S is the stress amplitude and S_0 and n are material constants. The second damping law concerns nonlinear damping for which

$$g = \left(\frac{S}{S_0} \right)^n \frac{\omega\tau}{1 + \omega^2\tau^2} \quad (\text{ii})$$

with the relaxation time τ being an additional material constant. Correlations provided by the scaling laws were performed on data from a large number of tests with steel, brass, and aluminum cantilever beams. The steel and brass data were correlated reasonably well on the basis of (i) while the aluminum data were better correlated on the basis of (ii).

NASA

where S is the stress amplitude and S_0 and n are material constants. The second damping law concerns nonlinear damping for which

$$g = \left(\frac{S}{S_0} \right)^n \frac{\omega\tau}{1 + \omega^2\tau^2} \quad (\text{ii})$$

with the relaxation time τ being an additional material constant. Correlations provided by the scaling laws were performed on data from a large number of tests with steel, brass, and aluminum cantilever beams. The steel and brass data were correlated reasonably well on the basis of (i) while the aluminum data were better correlated on the basis of (ii).

NASA

where S is the stress amplitude and S_0 and n are material constants. The second damping law concerns nonlinear damping for which

$$g = \left(\frac{S}{S_0} \right)^n \frac{\omega\tau}{1 + \omega^2\tau^2} \quad (\text{ii})$$

with the relaxation time τ being an additional material constant. Correlations provided by the scaling laws were performed on data from a large number of tests with steel, brass, and aluminum cantilever beams. The steel and brass data were correlated reasonably well on the basis of (i) while the aluminum data were better correlated on the basis of (ii).

NASA